Contents

0.1 Time-Varying Analysis of Brain Networks [0]

Typical neurophysiological recordings of the brain activity such as electroencephalography (EEG) or magnetoencephalography (MEG) are non-stationary signals. Time-frequency analysis is therefore a suitable tool for analysis of such signals. Over the years, time-frequency analysis has found numerous applications in computational neuroscience from the diagnosis of schizophrenia in adults (e.g., [1]) to understanding the autism spectrum disorder in a pediatric population [2]. With advances in computational resources and various imaging modalities, the time-frequency analysis is poised to become one of the main tools in the area of computational neuroscience.

Time-frequency analysis is especially critical in the analysis of brain networks, which represent the human brain as a complex network of interconnected nodes. Nodes can represent individual neurons or groups of neurons, as well as group of voxels obtained from magnetic resonance imaging (MRI), while edges correspond to the correlation or connectivity between these regions [3], [4]. Recent publications emphasized the fact that the properties of these networks can be used as diagnostic biomarkers for various diseases including but not limited to Alzheimer's diseases [5], stroke [6] and other brain disorders [7], [8].

0.1.1 Brain Networks

Brain networks typically denote networks of interconnected distinct units in the brain [4]. The units can represent individual neurons or anatomically distinct brain regions. In general, structural, functional and effective brain networks can be considered. Structural networks refer to networks describing structural (i.e., physical) connections between nodes (e.g., neurons). Functional networks refer to networks established to denote statistical dependence between nodes, regardless of whether the nodes are physically connected or not. The statistical dependence between nodes can be quantified using various approaches, from simple correlation to more advanced time-frequency, (t, f), based approaches. Effective networks usually correspond to directional networks where the relationships are determined through causality [4].

Brain networks are usually represented using graphs via a matrix format. That is, a matrix element, m_{ij}, represents the connection between the i^{th} and j^{th} nodes. To form these brain connection matrices, usually called connectivity matrices, we begin with neuroimaging data obtained via one of the modalities such as MRI, EEG, MEG or near infrared spectroscopy. Depending on the imaging procedure, structural or functional connectivity matrices are established next. Once connectivity matrices are established, graph theoretical tools are utilized to understand the

[0]Author: **Ervin Sejdić**, Department of Electrical and Computer Engineering, University of Pittsburgh, Pittsburgh, PA 15261, USA (esejdic@ieee.org). **Selin Aviyente**, Department of Electrical and Computer Engineering, Michigan State University, East Lansing, MI 48824, USA (aviyente@egr.msu.edu). **Boualem Boashash**, Department of Electrical Engineering, Qatar University, Doha, Qatar (boualem@qu.edu.qa). Reviewers: A.A and A. A.

network properties [4].

0.1.2 Time-Frequency Analysis for Brain Networks

The brain and its various functions represent a highly nonstationary system. The strength and the number of interconnections between brain regions continuously change which enables the (t, f) analysis to have a number of uses in the analysis of brain networks. Here, we outlined the main three cases.

0.1.2.1 Establishing Connectivity Matrices via Time-Frequency Analysis

Cross-correlation is typically utilized to assess the relationship between different brain regions. However, a simple correlation coefficient at the zeroth lag is limited in its ability to assess the interactions of these signals, as it can only quantify the linear relationships and capture mostly the amplitude based relationships. (T, f) tools become important in this case, and publications typically examine phase synchrony amongst neuroimaging signals representing different nodes. Synchrony measures relate two signals' temporal structures without considering their amplitude. Hence, any two signals are denoted synchronous as long as their rhythms (i.e., temporal structures) are similar. The degree of synchrony between two signals is usually assessed via estimation of instantaneous phase around a particular frequency. The estimation of instantaneous phase is usually accomplished via the Hilbert transform or (t, f) methods. Given that neuroimaging signals are predominantly nonstationary signals, (t, f) methods are more suitable for the calculation of synchrony between two signals [9]. Traditionally, a Morlet wavelet based method was used [10], but here we present a recently proposed method based on a quadratic (t, f) representation [9].

Let us consider a (t, f) representation of a signal based on the reduced interference Rihaczek (t, f) distribution (RID-Rihaczek) as defined in Chapter 3 (e.g., Table 3.3.2):

$$\rho_z(t,f) = \int\int \exp\left(-\frac{\theta^2\tau^2}{\sigma}\right) \exp\left(j\frac{\theta\tau}{2}\right) A(\theta,\tau)\exp(-\theta\tau - j\tau f)d\theta d\tau \qquad (0.1.1)$$

where $A(\theta, \tau)$ is the ambiguity function as defined in previous chapters (e.g., page 66, Chapter 3); $\exp(j\theta\tau/2)$ is the kernel for the Rihaczek distribution and $\exp(-\theta^2\tau^2/\sigma)$ is the Choi-Williams kernel used to reduced the effect of the cross-terms. Other kernels can be used as long as they remove the cross-terms in the Rihaczek amplitude spectrum. The next step is to estimate the time-varying phase in the (t, f) plane. This is accomplished via the following equation:

$$\Phi(t,f) = \arg\left[\frac{\rho_z(t,f)}{|\rho_z(t,f)|}\right] \qquad (0.1.2)$$

Using the definition of the time-varying phase spectrum, the phase difference between two signals, $z_1(t)$ and $z_2(t)$, can be similarly defined as follows:

$$\Phi_{12}(t,f) = \arg\arg\left[\frac{\rho_{z_1}(t,f)\rho^*_{z_2}(t,f)}{|\rho_{z_1}(t,f)||\rho_{z_2}(t,f)|}\right]. \qquad (0.1.3)$$

It should be mentioned that $\Phi(t,f)$ and $\Phi_{12}(t,f)$ are assumed to be zero for (t,f) points equal to zero.

Based on the estimate of a time-varying phase spectrum as shown above, a synchrony measure still needs to be defined. In this article, the phase locking value (PLV) is considered here. PLV can be defined between two signals and averaged across realizations/trials [9]:

$$PLV(t,f) = \frac{1}{TR}\left|\sum_{k=1}^{TR}\exp(j\Phi_{12}^{k}(t,f))\right| \tag{0.1.4}$$

where TR is the number of trials/realizations and $\Phi_{12}^{k}(t,f)$ is the time-varying phase estimate between two electrodes for the k^{th} trial. PLV measures the inter-trial/interrealization variations of phase differences at time t and frequency f. PLV close to 1 indicated small phase difference across trials/realizations. It should be noted that PLV is applied to neuroimaging signals between pairs of channels, i.e., it is a bivariate measure not a multivariate measure. Most neuroimaging experiments have multiple trials, but for single trials, a so-called single trial PLV is calculated denoting the consistency of the phase across time. Lastly, the described phase synchrony measure assesses the instantaneous phase differences between signals in the (t,f) domain [11].

0.1.2.2 Understanding The Time-Varying Nature of Brain Networks

The next challenge in the analysis of brain networks lies in the analysis of connectivity matrices. These connectivity matrices change over time. This is expected in many cases, especially when a person is performing repeated operations over a certain time span. A second possibility is the case when it is expected that activated brain nodes will changes over time due to a neurological disease or aging. However, to utilize (t,f) analysis for the examination of the time-varying nature of these brain networks, one needs to use spectral graph theory.

Let's consider undirected weighted graphs $\mathfrak{G} = \{\upsilon, \xi, W\}$ with υ is a finite set of vertices, N is the cardinality of υ, ξ is a set of edges and W is a weighted connectivity matrix. A signal $z : \upsilon \to \mathbb{R}^N$ defined on the vertices of the graph may be represented as a vector $z \in \mathbb{R}^N$, where the n^{th} component of the vector z represents the signal value at the n^{th} vertex in υ. Briefly, the classical Fourier transform expands of a signal in terms of complex exponentials that can be considered to be eigenfunctions of the one-dimensional Laplace operator: $-\triangle(\exp(j2\pi ft)) = (2\pi f)^2\exp(j2\pi ft)$. Using the same analogy, the graph Fourier transform of a function $z(n)$ can be defined in terms of the eigenvectors, $\chi(n)$, of the connectivity matrix Laplacian [12]:

$$Z(\lambda_l) := \langle z, \chi_l\rangle = \sum_{n=1}^{N} z(n)\chi_l^*(n) \tag{0.1.5}$$

with the inverse graph Fourier transform being equal to:

$$z(n) := \sum_{l=i}^{N-1} Z(\lambda_l)\chi_l(i) \tag{0.1.6}$$

The classical Fourier transform provides a unique interpretation of frequencies. When f is close to zero (i.e., low frequencies), the complex exponential functions are oscillating very slowly and are very smooth. However, when f is much greater than zero (high frequencies), the oscillations of the complex exponential functions become faster. Similarly, the graph Laplacian eigenvalues and eigenvectors can be interpreted as follows: The Laplacian eigenvector χ_0 is constant and equal to $1/\sqrt{L}$ at each vertex. The graph Laplacian eigenvectors associated with low frequencies λ_l, vary slowly across the graph, i.e., if two vertices are connected by an edge with a large weight, the values of the eigenvector at those locations are likely to be similar. The eigenvectors associated with larger eigenvalues oscillate more rapidly and are more likely to have dissimilar values on vertices connected by an edge with high weight [12].

Using the definition of the graph Fourier transform, the short-time graph Fourier transform of a function $z(n) \in \mathbb{R}$ can be given as [13]:

$$F_z^g(n,k) = \langle z, g_{i,k}(n) \rangle \tag{0.1.7}$$

where a windowed graph Fourier atom $g_{i,k}(n)$ is given as

$$g_{i,k}(n) = N\chi_k(n) \sum_{l=0}^{N-1} \widehat{g}(\lambda_l)\chi_l^*(i)\chi_l(n). \tag{0.1.8}$$

$\widehat{g}(\lambda)$ is a window definition in the graph spectral domain.

0.1.2.3 Time-Frequency Features of Time-Varying Networks

Time-varying networks can be analyzed using the vertex-frequency analysis, the graph analogous of the (t, f) analysis for one- or two-dimensional signals. As two-dimensional representation is obtained similar to a (t, f) representation, we can utilize some of the (t, f) tools developed for the analysis of (t, f) representations. In particular, we can calculate (t, f) features such as [14]:

- The energy concentration defined as

$$TFEC = \left(\sum_{n=1}^{N} \sum_{k=1}^{M} |S_x^g(n,k)|^{1/2} \right)^2 \tag{0.1.9}$$

- The (t, f) Renyi entropy given by

$$TFRE = \frac{1}{1-\alpha} \log_2 \left(\sum_{n=1}^{N} \sum_{k=1}^{M} \left(\frac{S_x^g(n,k)}{\sum_{n=1}^{N} \sum_{k=1}^{M} S_x^g(n,k)} \right)^{\alpha} \right) \tag{0.1.10}$$

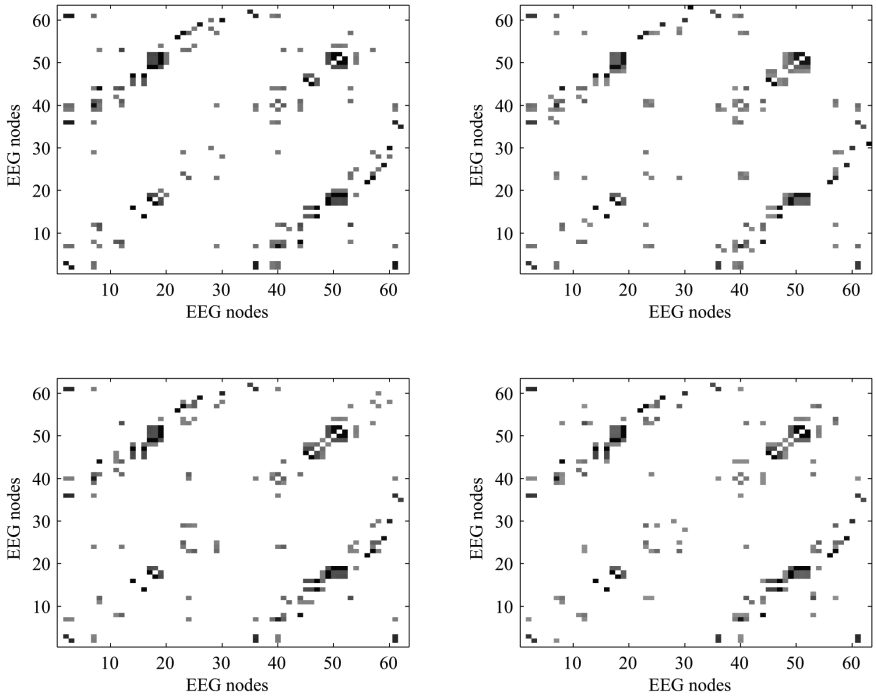

Fig. 0.1.1: Brain networks for sample four swallows.

- Time-varying spectral flatness

$$TFSF = -\frac{1}{NM}\sum_{n=1}^{N}\sum_{k=1}^{M} S_x^g(n,k)\log_2 S_x^g(n,k) \tag{0.1.11}$$

where $S_x^g(n,k) = |F_x^g(n,k)|^2$ is the spectrogram of the considered signal and $\alpha = 3$ is a typical value for TFRE. There are many more (t,f) features that can be utilized in the analysis. It should be pointed out that if a (t,f) distribution can be considered as an image (e.g., all points are greater or equal to zero), then features considered in image processing applications can be considered here as well.

0.1.3 Illustrating Examples

As an illustrating example of the proposed approach, let us consider a sample EEG recording from a healthy adult participant performing four saliva swallows in the head neutral position. The sample signals were collected from 64 EEG electrodes positioned according to the 10-20 international electrode system. Electrode positioning was accomplished using the actiCAP active electrodes (BrainProducts, Germany), and signal amplification was performed using the actiCHamp amplifier

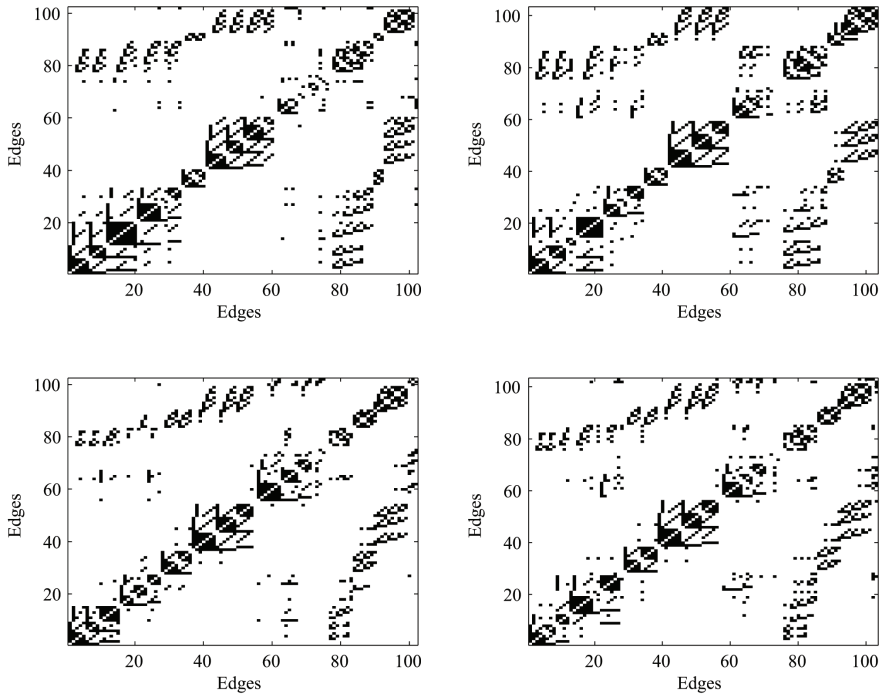

Fig. 0.1.2: Line graphs of brain networks for the four swallows.

(BrainProducts, Germany). The P1 electrode was chosen as the reference (i.e., EEG voltage potentials are referenced to P1). During the course of all data collections, the electrode impedance was below 15 kΩ. The PyCorder acquisition software provided a 10 kHz sampling frequency, and it was also used for saving collected data on a computer hard drive.

To establish brain connectivity matrices, we utilized equations (0.1.3) and (0.1.4) to calculate bivariate phase differences and corresponding PLV values for all EEG channels. The computed connectivity matrices are not sparse, as many spurious connections also appear. Therefore, to concentrate on most relevant connections, we thresholded connectivity matrices to keep only 5% of the strongest connections. The established brain connectivity matrices for four swallows are shown in Figure 0.1.1. Even though the swallows are from the same healthy participant, differences in the established networks can be observed in the presented networks. It is obvious that even though most of the functional connections are present for all swallows, there are swallow-by-swallow differences even in healthy individuals, which need to be further quantified. While typical network metrics such as clustering coefficients or global efficiency measures can be calculated, those metrics do not reveal any information about the time-varying nature of these brain networks. Specifically,

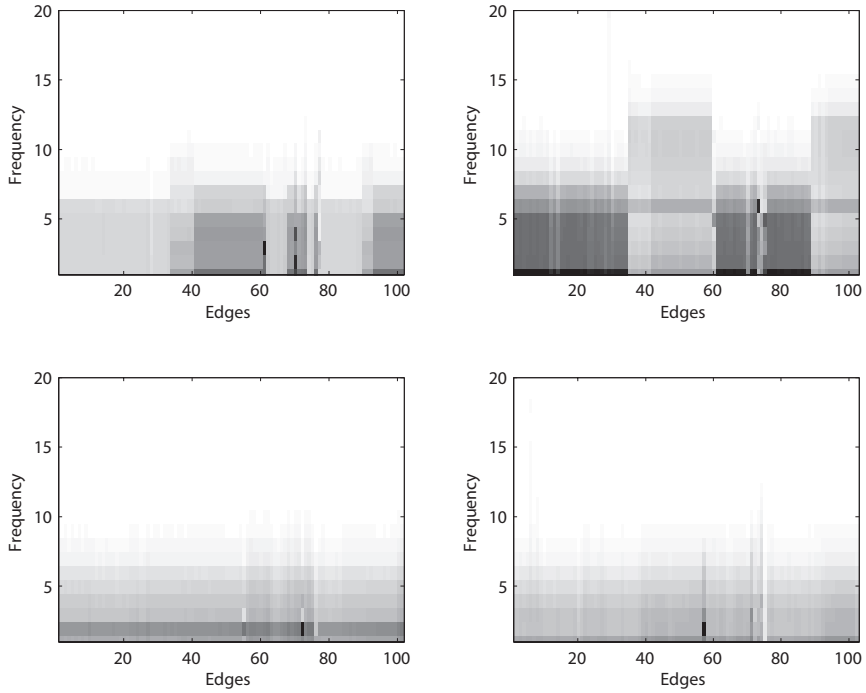

Fig. 0.1.3: Edge-frequency representations of four swallows.

even though the values of these network metrics can be different on a swallow-by-swallow basis, we do not have any details how the networks have changed. Therefore, it would be beneficial to apply the vertex-frequency analysis in order to understand the time-varying changes in the swallowing networks.

For the vertex-frequency analysis to be applicable to these networks, time-varying data points need to be on vertices. Hence, as the changes here are in the actual connections (i.e., edges), one needs to convert the considered network representations into line graphs. In other words, edges becomes vertices which are connected by unity edges. Such conversions yield edge-connectivity matrices as shown in Figure 0.1.2. These edge-edge connectivity matrices are then used to calculate edge-frequency representations via equations (0.1.7) and (0.1.8). These representations, as shown in Figure 0.1.3, depict spectrograms of the brain networks shown in Figure 0.1.1. The obtained representations clearly depict the time-varying nature of the swallowing networks, as the frequency content of the networks changes on a swallow-by-swallow basis.

Next, we would like to quantify these changes by examining the three (t, f) features outlined in the previous section. Our results for the four sample swallows are outlined in Table 0.1.1, which are calculated from the network spectrograms. As

Table 0.1.1: Values of the three (t, f) features.

	SW1	SW2	SW3	SW4
TFED	0.562	0.754	0.396	0.494
TFRE	8.958	9.394	8.886	8.924
TFSF	7274	5206	3532	4612

these features clearly capture the differences in the edge-frequency representations, we can state that features based on (t, f) representations (or more specifically, edge-frequency representations) are suitable to understand differences in brain networks during the four swallowing actions. The presented results are just sample results that demonstrate the applicability of typical (t, f) measures in the network analysis. Future works should investigate the relationships between typical network metrics and (t, f) features. Those investigations will provide us with more understanding about the utility of the (t, f) network analysis.

0.1.4 Summary and Conclusions

In this article, we briefly described the utilization of the (t, f) analysis in modern computational neuroscience applications. Specifically, we considered the application of the (t, f) analysis to the analysis of brain networks. The (t, f) analysis is very suitable for the establishment and post-analysis of the established brain networks. We concluded the article with an illustrative example.

References

[1] M.-E. Lynall, D. S. Bassett, R. Kerwin, P. J. McKenna, M. Kitzbichler, U. Muller, and E. Bullmore, "Functional connectivity and brain networks in schizophrenia," *The Journal of Neuroscience*, vol. 30, pp. 9477–9487, July 2010.

[2] J. Peters, M. Taquet, C. Vega, S. Jeste, I. Fernandez, J. Tan, C. Nelson, M. Sahin, and S. Warfield, "Brain functional networks in syndromic and non-syndromic autism: a graph theoretical study of EEG connectivity," *BMC Medicine*, vol. 11, pp. 54–1–16, Feb. 2013.

[3] M. Rubinov and O. Sporns, "Complex network measures of brain connectivity: Uses and interpretations," *NeuroImage*, vol. 52, pp. 1059–1069, 3 2010.

[4] E. Bulmore and O. Sporns, "Complex brain networks: graph theoretical analysis of structural and functional systems," *Nature Reviews Neuroscience*, vol. 10, pp. 186–198, Mar. 2009.

[5] C. J. Stam, W. de Haan, A. Daffertshofer, B. F. Jones, I. Manshanden, A. M. van Cappellen van Walsum, T. Montez, J. P. A. Verbunt, J. C. de Munck, B. W. van Dijk, H. W. Berendse, and P. Scheltens, "Graph theoretical analysis of magnetoencephalographic functional connectivity in Alzheimer's disease," *Brain*, vol. 132, pp. 213–224, Jan. 2009.

[6] C. Grefkes and G. R. Fink, "Reorganization of cerebral networks after stroke: new insights from neuroimaging with connectivity approaches," *Brain*, vol. 134, pp. 1264–1276, May 2011.

[7] P. J. Uhlhaas and W. Singer, "Neural synchrony in brain disorders: Relevance for cognitive dysfunctions and pathophysiology," *Neuron*, vol. 52, pp. 155–168, Oct. 2006.

[8] P. J. Uhlhaas and W. Singer, "Abnormal neural oscillations and synchrony in schizophrenia," *Nature Reviews Neuroscience*, vol. 11, pp. 100–113, Feb. 2010.

[9] S. Aviyente, E. M. Bernat, W. S. Evans, and S. R. Sponheim, "A phase synchrony measure for quantifying dynamic functional integration in the brain," *Human Brain Mapping*, vol. 32, pp. 80–93, Jan. 2011.

[10] J.-P. Lachaux, E. Rodriguez, J. Martinerie, and F. J. Varela, "Measuring phase synchrony in brain signals," *Human Brain Mapping*, vol. 8, no. 4, pp. 194–208, 1999.

[11] S. Aviyente and A. Y. Mutlu, "A time-frequency-based approach to phase and phase synchrony estimation," *IEEE Transactions on Signal Processing*, vol. 59, pp. 3086–3098, July 2011.

[12] D. I. Shuman, S. K. Narang, P. Frossard, A. Ortega, and P. Vandergheynst, "The emerging field of signal processing on graphs: Extending high-dimensional data analysis to networks and other irregular domains," *IEEE Signal Processing Magazine*, vol. 30, pp. 83–98, May 2013.

[13] D. I. Shuman, B. Ricaud, and P. Vandergheynst, "Vertex-frequency analysis on graphs," *ArXiv e-prints*, 2013.

[14] B. Boashash, G. Azemi, and J. M. O'Toole, "Time-frequency processing of nonstationary signals: Advanced TFD design to aid diagnosis with highlights from medical applications," *IEEE Signal Processing Magazine*, vol. 30, pp. 108–119, Nov. 2013.